

LASING CHARACTERISTICS OF YTTERBIUM, THULIUM AND OTHER
RARE-EARTH DOPED SILICA BASED FIBERS

P.J.Suni¹, D.C.Hanna, R.M.Percival, I.R.Perry,
R.G.Smart, J.E.Townsend and A.C.Tropper

Physics Department
† Department of Electronics and Computer Sciences
Southampton University
Southampton SO9 5NH
United Kingdom

ABSTRACT

We have experimentally studied the lasing characteristics of silica fibers doped with Yb, Tm, Pr and Ho and present a summary of these results.

1. INTRODUCTION

Rare-earth doped fiber lasers have in recent years received increased attention in the literature. To date most of the attention has been focused on erbium and neodymium doped fibers, primarily because of their promise as direct optical amplifiers in the two important communications bands near $1.5\mu\text{m}$ and $1.3\mu\text{m}$, respectively. While much of the commercial interest is likely to remain in the area of optical communications amplifiers based on Er^{3+} and Nd^{3+} , it is also important to realize that five other rare-earths have successfully been incorporated into silica hosts and operated as fiber lasers. These may find use in other application areas, such as distributed sensors and superfluorescent sources. Furthermore, fiber lasers are showing promise not only as fairly low power devices, with typical power levels of the order of several mW, but may also be operated at significantly higher power levels. Output powers of 120mW from a laser diode-pumped Nd-doped fiber at $1.0\mu\text{m}$, 99mW from an argon pumped Er-doped fiber at $1.55\mu\text{m}$ have previously been demonstrated and we report here 50mW of power at $2.0\mu\text{m}$ from a Tm-doped fiber pumped by a cw Nd:YAG laser. There is no reason why these powers should not be scalable to much higher values. When such power levels are considered together with the other features that are hallmarks of glass lasers in general and fiber lasers in particular, namely wide choice of laser wavelengths, diode pumpability (in many cases) and tuning ranges varying from tens to well in excess of one hundred nanometers, it becomes clear that these lasers may find new uses, e.g. as spectroscopic sources or for medical and lidar applications.

¹ Present address: Coherent Technologies, Inc., P.O.Box 7488, Boulder, CO 80306

A convenient way of summarizing the wavelength coverage of fiber lasers to date is shown in figure 1. The top part shows all laser wavelengths that have been demonstrated in silica fibers that are known to us. The width of each bar indicates the tuning range that has been achieved. Wavelengths range from 651nm in Sm to beyond 2 μ m in Tm and Ho.

It is also worthwhile to note that the use of a glass host other than silica may significantly affect the position, linewidth, strength and lifetime of a particular transition. In particular, recent interest has been focused on fluoro-zirconate glasses which have lower phonon energies than silica (and hence lower nonradiative decay rates in the infrared beyond 2 μ m) and are transparent in the 2-3 μ m region where silica begins to absorb strongly. Significant technical problems have prevented the production of fibers with diameters smaller than about 15 μ m at present and hence fluoride based fiber lasers are in most cases multimode devices. Typically this means that laser thresholds are higher than those of silica fibers. Nevertheless, demonstrations of laser action have been made with several dopants. The lower half of figure 1 shows the wavelengths where laser action has been demonstrated in fluoro-zirconate fibers. Of particular interest is lasing on the $^4F_{3/2}$ - $^4I_{13/2}$ transition at 1.38 μ m in Nd³⁺, a transition which suffers from excited state absorption (ESA) in silica, and emission as far out as 2.7 μ m on the $^4I_{11/2}$ - $^4I_{13/2}$ transition in Er³⁺. Laser action on the latter transition does not occur in silica, in part because nonradiative decay severely shortens the upper laser level lifetime. These cases clearly demonstrate the important influence of the host on the laser performance. Much work remains to be done in the area of fluoro-zirconate and other hosts.

During the past two years we have carried out experimental work on four rare-earths (Yb, Tm, Pr and Ho) and we present here a summary of the laser performance obtained to date. Both Yb and Tm have shown very promising results, whereas Pr and Ho have so far been less efficient. We discuss some reasons for the differences and some potential routes to improvements.

In the discussion of the various laser systems the following points should be noted:

All fibers discussed were fabricated by the Optical Fiber Group at Southampton University. The host glass has in all cases been silica based because of the particular fabrication facilities available at Southampton University. The Yb and Tm fibers were fabricated by the solution doping technique, whereas the Pr and Ho fibers were made by the MCVD technique, several years ago. Emission spectra were recorded by monitoring fluorescence emitted perpendicular to the fiber in order to avoid reabsorption of parts of the spectrum. These spectra have not been corrected for monochromator and/or detector response. In all cases pumping was done through microscope objectives and laser cavities consisted of

two mirrors butted to the fiber ends. The input mirror always had high (typically 70-90%) transmission at the pump wavelength and high reflectivity ($R > 99\%$) at the laser wavelength. Table 1 summarizes the relevant data on the various fibers used.

TABLE 1

Dopant	Concentration (ppm)	N.A.	Diameter (μm)	Cut-off (nm)
Yb	580	0.16	3.7	800
Tm	740	0.15	8.6	1700
Pr	450	0.26	2.5	890
Ho	200	0.21	8.0	2160

2. YTTERBIUM

Ytterbium¹⁰⁻¹³ is an interesting dopant for several reasons. The energy level structure (shown schematically in figure 2) is extremely simple in comparison with many other rare-earths, consisting of a split ground state $^2F_{7/2}$ and a split excited state $^2F_{5/2}$. The lack of other energy levels in the infrared and the visible ensures that ESA will not be a problem and hence the results presented below on efficiency and output power should be scalable to much higher values.

Ytterbium is also interesting because of its emission spectrum, which consists of two broad peaks (see figure 2). The peak centered at 974nm (transition A) corresponds to a pure 3-level laser transition directly to the ground state and has a width of 10nm FWHM. This emission is potentially useful as a pump source for Er-doped fibers.¹⁴ The second peak centered at 1036nm (transition B) has a width of 50nm. Laser action on this transition is nearly 4-level in nature. Tuning over a very wide range has been obtained on this transition.

In addition to achieving laser oscillation on these two transitions, we have also demonstrated that very efficient superfluorescent (amplified spontaneous emission) operation can be achieved. Such emission is of particular interest in cases, such as laser gyros, where broadband light is required, but where the mode structure of a normal laser oscillator cannot be tolerated.

Ytterbium has a high enough gain that under proper pump conditions the 3.5% Fresnel reflection from the cleaved output end of the fiber can provide enough feedback to give very efficient laser operation. Pump light at 900nm was used to establish oscillation at 974nm in a 0.5m long fiber. This detuning from the absorption peak at 910nm was found to give more output power due to the

higher pump power available at this wavelength. Longer lengths of fiber ($\sim 1\text{m}$) resulted in oscillation on the second emission peak at 1036nm. The reason for this switch is that oscillation at 974nm requires a much larger population in the upper laser level in order for inversion to occur throughout the fiber than is required for inversion with respect to the 1036nm transition. Excessive lengths of fiber means that the pump power is not inverting the output end of the fiber and hence leads to reabsorption losses of the emitted light. The optimum length of fiber for a 3-level laser is that which reduces the pump power to the saturation power at the output end. By saturation power we mean the power needed to excite half the ions into the upper laser level. For a 4-level laser reabsorption does not occur and hence the fiber length is not important. Optimum results occur for lengths such that all the pump light is absorbed.

The maximum output power at 974nm was 9.3mW for an absorbed pump power of 25.3mW and the threshold absorbed power was 11.5mW. The slope efficiency with respect to absorbed power was 67%. We note that Armitage et al.¹² have also reported lasing on this transition with a slope efficiency of 80%. In the case of the 1036nm emission, maximum output power was 15.7mW for 30.6mW absorbed with a threshold absorbed power of 9.4mW. The slope efficiency with respect to absorbed power was 77%. We also note that with less output coupling laser emission has been observed on the 4-level transition when pumped as far down as 800nm, over 100nm away from the absorption peak.

To observe superfluorescence we used the same experimental set-up, except that the output end of the fiber was immersed in index-matching liquid in order to suppress Fresnel reflections back into the fiber. The length dependence of the emission wavelength follows similar considerations to those above for laser emission: for output on the three level transition to dominate, the fiber absorption must be bleached throughout its length. To investigate the length dependent behaviour the fiber was progressively cut back while measuring the amount of superfluorescence on transitions A and B as well as the residual pump power at the fiber output. Approximately 30mW of pump power at 900nm was launched into the fiber for these measurements. Output power versus fiber length is shown in figure 3. We see that for short lengths the 3-level emission at 974nm predominates, whereas for lengths greater than about 0.75m the 4-level emission around 1040nm is favoured. We note that the peak in the 974nm emission occurs where the residual pump power is about 5mW, approximately equal to the calculated saturation power.

Figure 3 shows that the optimal fiber length for emission at 974nm is 0.5m when pumped with 30mW launched power. Using this length, the fiber yielded 10mW of superfluorescent output at 974nm when pumped at slightly higher powers. The slope efficiency in the high output power regime was about 45%. For the four level transition the choice of fiber length is again not critical. Since maximum

pump power from the dye laser was available at 850nm, we used this pump wavelength and a 5m length of fiber to ensure complete absorption of the pump power. This arrangement discriminated against the 974nm emission since the small absorption cross-section, and hence high saturation intensity, at 850nm reduced the inversion of the three level transition. The maximum output power was 31mW with a slope efficiency of about 45%.

The bandwidth (FWHM) of the 974nm emission was measured as 2nm, but the four level bandwidth and indeed linecentre position exhibited a dependence on both pump power and wavelength. In the high power regime (70mW absorbed at 850nm) the emission was centered at 1040nm with a 20nm bandwidth. The wavelength increased with decreasing power such that at very small output levels it had shifted to 1049nm with a bandwidth of 25nm. Pumping at 900nm reduced the bandwidth to 9nm for high power pumping. We believe that these effects may be due to site-dependent effects and will be investigated further.

The laser tuning range of the broad 4-level fluorescence was investigated using the resonator shown in figure 4. Approximately 100mW of pump light at 840nm was launched into a 3m length of fiber. The particular pump wavelength was chosen to simulate pumping with a high-power GaAlAs diode laser. The output end of the fiber was terminated in an index-matching cell to prevent lasing off the fiber end-face. This precaution is particularly important for tuning in the wings of the transition where the emission cross-section is small compared with line center. The resonator uses two prisms as the dispersing element. One prism was found not to provide sufficient dispersion to prevent simultaneous laser action at more than one wavelength. Feedback was provided by a second high reflector which could be rotated through small angles to select the laser wavelength. The low output coupling of the mirrors meant that it was necessary to extract laser output in the form of a reflection from the first prism. A polarisation controller, as described elsewhere¹⁵, was also found to be necessary in order to compensate for small amounts of birefringence in the fiber and provide a linear polarisation to match the near Brewster angle of the prisms.

The resulting tuning curve is shown in figure 4. Laser action was observed continuously over the range 1010-1162nm at room temperature. By immersing the fiber in liquid nitrogen the lower wavelength limit could be extended down to 1000nm due to the reduction in the thermally excited population of the lower laser level, thus reducing self-absorption at short wavelengths. The typical incident power threshold for the room temperature laser was about 60mW. Since the feedback mirror was essentially a total reflector, the output power from this mirror was only about 3μW over most of the tuning range. The output power could be greatly increased by decreasing the cavity losses (currently dominated by losses in the intracavity microscope objective) and by optimising the output coupling.

3. THULIUM

By comparison with ytterbium, thulium^{5,16-18} has a very much more complicated energy level structure (see figure 5). Laser action in a Tm-doped fiber can be achieved by pumping into one of several available absorption bands, each having its own advantages and disadvantages. While it is possible to pump Tm with an argon laser this is less attractive except in a laboratory environment. Furthermore it has been shown by Millar et al.¹⁹ that Tm is susceptible to color center formation when pumped at such short wavelengths. We have observed lasing following pumping into the band centered near 660nm using a DCM dye laser. The efficiency of the laser was rather poor and is believed to be due to significant ESA. A much more attractive absorption band is centered near 785nm, where high power laser diodes are available, corresponding to absorption from the H_6 ground state to the F_4 level. In our experiments a Styryl 9M dye laser was used to simulate pumping by a laser diode. We have also pumped the fiber into the short wavelength wing of the H_6 to H_5 transition using a Nd:YAG laser at 1064nm.⁵ This pump wavelength is of particular interest because of the wide availability of high power Nd:YAG lasers.

The fluorescence spectrum of Tm^{3+} under excitation at 800nm is shown in figure 6. The curve labelled end-light shows the emission spectrum exiting the end of a 27cm length of fiber; that labelled side-light shows the spectrum emitted perpendicular to the fiber axis. The difference between the curves is due to reabsorption of light emitted at the short wavelength end in the end-light spectrum. The most striking feature of these curves is the very large linewidth of the $H_4 - H_6$ transition. A weak second peak at $\approx 1.4\mu m$ is resolved in end-light. We believe this corresponds to emission from the F_4 level to the H_4 level.

In our experiments using the dye laser as the pump source, pumping at 797nm led to optimum performance. This wavelength represents a compromise between pumping near the absorption line centre and maximising the available pump power. The best results were obtained with a 27cm length of fiber and 3% output coupling. Laser threshold occurred at 21mW of pump power launched into the fiber with emission at $1.94\mu m$. A slope efficiency, with respect to absorbed power, of 13% was measured. The maximum extracted power in this configuration was 2.7mW.

In order to achieve efficient laser action when pumping at 1064nm several factors must be taken into account. As is evidenced by a strong blue glow, ESA is rather efficient at this pump wavelength. To minimize the detrimental effects of ESA requires that the upper laser level population is kept to a minimum. This in turn requires a very low overall cavity loss. We used an output coupler whose transmission in air was measured to be 1% - this value may change when butted against a cleaved fiber end. Since the laser

efficiency is proportional to the ratio of the output coupling to the overall loss, it is clear that efficient operation requires that other cavity losses be kept very small. We did, in fact, note that our results were highly dependent on the quality of the fiber cleave. Cleave quality was inspected using an interferometer and only cleaves with a fringe or less of nonuniformity across the $125\mu\text{m}$ fiber gave reasonably high efficiencies. Furthermore, we noted a strong output power dependence on the fiber length, with optimum results occurring with a 1.75m length. This is despite the fact that laser oscillation occurred at 2038nm , where the Tm system is essentially 4-level in nature. We believe that this length dependence is due to scattering and absorption losses which must be kept well below 50dB/km if they are not to significantly degrade the laser performance.

The prospect of mirror coating damage due to the high pump intensity at the fiber input limited the incident pump power to 1W . We found the threshold for laser action to occur at 60mW absorbed pump power and the slope efficiency (with respect to absorbed power) was 30%. For an incident power of 1W (450mW launched, of which 230mW was absorbed) the maximum laser output power was 51mW .

It is interesting to speculate on how much $2\mu\text{m}$ power one might be able to extract from a Tm fiber laser. If fiber losses are reduced to a negligible level one should be able to use a long enough length to absorb all the pump light. The input mirror damage problem may be circumvented by utilizing e.g. a double-clad fiber geometry²⁰ which allows pumping with a beam diameter much larger than the core size. This geometry would also reduce the pump intensity at the input end, thus reducing the effects of ESA and hence relaxing the low cavity loss requirement. Given that such a fiber could be efficiently pumped with a multimode $\text{Nd}:\text{YAG}$ laser, which are available at power levels of several tens of watts cw, it does not seem unreasonable to predict output powers of a watt, or even significantly more, from a single mode fiber.

Tuning of the Tm laser has been achieved by using a cavity similar to the one used to tune Yb , except in this case a 3-plate birefringent tuner from a commercial dye laser was used as the tuning element. The best results were achieved with pumping at 800nm . Because of the strong ESA rather poor tuning performance was observed when pumping at 1064nm . Improvements to this situation would require a tuning element that could be incorporated into the cavity without significantly adding to the cavity loss.

Initial tuning measurements were made with a 2.2m length of fiber. With this length the minimum incident threshold for laser oscillation was found to be 80mW . This laser could be tuned from $1.82\mu\text{m}$ to $2.056\mu\text{m}$. The tuning curve is shown in figure 7. The maximum extracted power was $\approx 100\mu\text{W}$ for an incident power of 210mW at 800nm . Significantly higher output powers should be possible

with a lower loss resonator and with optimised output coupling. Cutting back the fiber to 60cm led to the tuning curve shifting towards shorter wavelengths as a result of reduced self-absorption losses at short wavelengths. The long wavelength limit of this tuning curve is less than that for the 0.6m case as there is less pump power absorbed in the fiber for the shorter length.

Mention has been made of the strong ESA when pumped at several wavelengths. In fact, one of the striking features of Tm-doped silica is the rather strong blue emission which results when pumped e.g. at 650nm or 1064nm. The emission emanates from the 1D_2 and 1G_4 levels which radiate near 460nm and 475nm, respectively. We have also detected UV emission at 370nm from the 1D_2 level directly to ground. To the eye the blue emission appears so strong that one is led to speculate about the possibility of producing an upconversion fiber laser, i.e. laser action at a wavelength shorter than the pump wavelength. Unfortunately this is an unlikely prospect in silica fibers even though the lifetimes of both 1D_2 and 1G_4 are $>100\mu s$. Even under very strong pumping we have estimated that only of the order of 10^{-6} of the ground-state population is promoted to these higher lying states. The main limitation in silica are the short lifetimes of the intermediate levels which must be populated in a multistep absorption of pump photons.

The upconversion process is likely to be much more efficient in fluoride hosts, where lifetimes are typically an order of magnitude longer than in silica. While this is good news as far as upconversion goes it may, on the other hand, make laser action at $2\mu m$ more difficult to achieve.

4. PRASEODYMIUM

Trivalent praseodymium^{21,22} is an interesting laser activator because its energy level spectrum (see figure 8) contains an exceptionally large number of metastable multiplets ($^3P_{2,1,0}$, 1D_2 , 1G_4) from which laser action has been demonstrated in crystalline hosts at various wavelengths from the visible²³, to the near infra-red.²⁴

Laser action in a praseodymium-doped silica fiber was first reported by Reekie et al.²¹, who observed emission at 1080nm when pumping at 590nm using a Rhodamine 6G dye laser. The authors suggested that the $^1G_4 - ^3H_4$ (ground multiplet) transition was responsible, as in for example the crystalline $Pr^{3+}:CaWO_4$ system. Because several of the fluorescence bands in silica are very broad (see figure 9) and contain spectrally overlapping contributions from more than one initial level, the assignment of transitions is difficult. Based on spectroscopic measurements published

elsewhere²² and on the observation by Ainslie et al.²⁵ that the emission band at $\approx 1\mu\text{m}$ will contain overlapping contributions from the $^1\text{D}_2 - ^3\text{F}_{4,3}$ and $^1\text{G}_4 - ^1\text{H}_4$ transitions, we believe that the upper laser level is most likely $^1\text{D}_2$ rather than $^1\text{G}_4$.

We have achieved laser action at both 1080nm and 888nm in the same Pr-doped silica fiber that was used in reference 21. The absorption spectrum of the fiber contains three bands in the 400-1100nm region corresponding to the $^1\text{H}_4 - ^3\text{P}_{0,1,2}$, $^1\text{D}_2$, and $^1\text{G}_4$ transitions at 450-490nm, 580-590nm, and 970-980nm respectively²⁵

To investigate the laser performance on the $^1\text{D}_2 - ^3\text{F}_{3,4}$ and $^1\text{D}_2 - ^3\text{F}_2^3\text{H}_6$ transitions we pumped a 1.3m length of fiber using a Rhodamine 6G dye laser at 590nm. Argon laser pumping at 488nm was investigated as well, but led to much poorer results. With 2% output coupling the absorbed power threshold for laser action at 1080nm was $\approx 2\text{mW}$. Since the cavity contained no spectrally selective elements, lasing occurred at several wavelengths over a range of 10nm centered at 1080nm. Changing the output coupling to 14% raised the laser threshold to 5mW but resulted in a higher slope efficiency (5%) and higher output powers - up to 1.7mW.

To observe laser operation on the 888nm transition a pair of mirrors with reflectivity $>99.5\%$ at 888nm and a transmission of $\approx 90\%$ at 1080nm were used. The threshold for stimulated emission on this transition was then found to be $\approx 10\text{mW}$ of absorbed power with overall cavity losses measured to be 2%. Again lasing occurred at several wavelengths over a range of $\approx 10\text{nm}$, this time centered at 888nm. The relationship of output laser power and absorbed pump power was not investigated for this transition as no suitable output coupler was available.

Either of these transitions in principle offers a tunable range of at least 50-60nm. However, our results indicate that the overall (pump and radiative) quantum efficiencies of the two laser transitions are as low as 2% (1080nm) and 0.7% (888nm), suggesting that the radiative quantum efficiency for the $^1\text{D}_2$ multiplet is low. This makes the laser threshold rather high, especially with intracavity tuning elements, and the laser action rather inefficient.

For both these transitions the threshold for stimulated emission could be reduced by $\approx 30\%$ by immersing all but a few centimeters of fiber in liquid nitrogen. A number of processes may contribute to this, the most significant is probably an improvement in the radiative quantum efficiency at low temperatures.

5. HOLMIUM

Holmium²⁶ doped glass lasers were operated as early as 1962 by Gandy and Ginther.²⁷ The first operation of a fiber laser incorporating Ho was made by Brierley et al.²⁸ who used a fluorozirconate base glass. The relatively large fiber diameter (40 μ m) resulted in a rather high threshold. We have recently demonstrated laser action in a silica-based fiber doped with holmium.²⁵

Holmium has a strong absorption band between 450nm and 460nm and much weaker bands near 540nm and 650nm (see figure 10). Since the Ho system is a quasi-3-level system (the lower laser level has a significant thermal population at room temperature) pumping will be most efficient where the absorption cross-section is the largest, in order to minimise the fiber length and hence reabsorption of the emitted light. Consequently we have to date achieved lasing when pumping at 458nm, but not when pumping into the other, weaker, absorption bands.

Figure 11 shows a plot of the fluorescence spectrum exiting the end of the 50 cm length of fiber used in our experiment. As is typical the fluorescence band is quite wide and a significant tuning range is in principle possible, although we have not attempted such an experiment in the Ho case.

Laser oscillation at 2.04 μ m was achieved using the argon laser at 457.9nm to pump a short length of fiber. The 17cm fiber length used was the shortest that could be accommodated in our particular experimental arrangement. With this length of fiber 97% of the launched power was absorbed. With longer lengths threshold could not be reached, probably as a result of the greater self-absorption losses on this quasi-3-level transition. Shorter fiber lengths or lower doping levels may improve the performance somewhat.

The absorbed pump power for laser threshold was measured to be 46mW (95mW incident) using an output coupler with 2% transmission at the laser wavelength. The slope efficiency was measured to be 1.7% with respect to absorbed pump power with a maximum extracted power of 0.67mW for an absorbed power of \approx 85mW.

6. DISCUSSION

As we have shown the performance of fiber lasers varies significantly depending on the particular dopant in question. Particularly good performance has been achieved with ytterbium. Thulium has also been seen to operate quite efficiently under appropriate conditions. Holmium and praseodymium, on the other hand, have not operated as well as expected.

The parameter that contributes most strongly to this variation in performance is the radiative quantum efficiency η_q , i.e. the fraction of ions in the upper laser level that decay by radiation, rather than by nonradiative routes. The quantum efficiency can be calculated simply as the ratio of the fluorescence lifetime to the radiative decay time. The former is easily measured by chopping the pump beam and measuring the decay time of the fluorescence. The latter cannot be measured, but can for transitions terminating on the ground state be calculated by integrating the absorption spectrum over the transition in question.²⁹ Certain assumptions go into this calculation; in particular one assumes that all Stark levels are equally populated. This is not the case in several of our glasses. While ignoring such discrepancies may contribute to uncertainties in the calculated radiative decay rates we nevertheless believe that our estimates of η_q are reasonably accurate.

We first made test calculations on several systems which are known to have almost unity quantum efficiency - ytterbium and erbium-doped silica as well as thulium-doped fluorozirconate glass (bulk sample). In all cases the calculated radiative rates were consistent with $\eta_q \approx 1$. We then repeated the calculations for our Tm, Pr and Ho-doped fibers and found η_q to be 6%, <2% and 1.5%, respectively.

While these figures explain the rather poor performance of Pr and Ho, it is not clear at this point why the quantum efficiency is so low. We have investigated Tm in some detail to try to get some clues. Measurements have shown that for concentrations ranging from 58ppm to several thousand ppm there is no significant change in the fluorescent lifetime; this would seem to suggest that clustering of the dopant ions, which has been seen to lead to reduced quantum efficiency at high doping levels in Nd³⁺, is not playing a significant role here. Water concentrations have varied significantly in the samples, but again lifetime has not shown any particular trend with concentration. Calculations of multiphonon decay rates for a number of glasses have been made by Reisfeld et al.³⁰ These calculations have not been made for silica, but for glasses with similar phonon energies, nonradiative decay rates are small enough that they do not significantly reduce the quantum efficiency.

7. CONCLUSION

We have discussed several rare-earth doped silica fibers and shown that efficient performance can be achieved, particularly in Yb and Tm. We believe that the poor performance of Pr and Ho is mainly due to a very low radiative quantum efficiency in silica, but we

can at this point not offer an explanation of why this is so. On the other hand these poorly performing systems vindicate the fiber geometry. Continuous-wave laser action in a glass with less than a percent quantum efficiency would be unthinkable in a bulk system.

We also note, finally, that if the problem of the low quantum efficiency can be solved, then the laser performance of the Tm, Pr and Ho-systems described can be expected to improve dramatically.

8. ACKNOWLEDGEMENTS

Funding for this work, including research fellowships (RMP, PJS) and several studentships (IRP, RGS and JET), was provided by the UK Science and Engineering Research Council, in part under the JOERS programme. The Pr and Ho fibers used were fabricated by Dr.S.B.Poole, formerly with the Optical Fibre Group at Southampton University.

9. REFERENCES

1. M.C.Farries, M.E.Fermann, R.I.Laming, S.B.Poole and D.N.Payne, "Distributed temperature sensor using Nd³⁺-doped optical fibre", *Electr. Lett.*, 22, 418-419, 1986
2. K.A.Fesler, B.Y.Kim and H.J.Shaw, "Fibre gyro experiment using fibre laser source", *Electr. Lett.* 25, pp. 534-536, 1988
3. H.Po, E.Snitzer, R.Tumminelli, L.Zenteno, F.Hakimi, N.M.Cho and T.Haw, "Double clad high brightness Nd fiber laser pumped by GaAlAs phased array", postdeadline paper PD7, OFC'89, Houston, 1989
4. M.S.O'Sullivan, J.Chrostowski, E.Desurvire and J.R.Simpson, "High power narrow linewidth erbium-doped fiber laser", paper TuP3, CLEO, Baltimore, 1989
5. D.C.Hanna, M.J.McCarthy, I.R.Perry and P.J.Suni, "Efficient high power continuous-wave operation of a monomode Tm-doped fibre laser at 2 μ m pumped by a Nd:YAG laser at 1.064 μ m", submitted to *Electr. Lett.*
6. W.J.Miniscalco, L.J.Andrews, B.A.Thompson, R.S.Quimby, L.J.B.Vacha and M.G.Drexhage, "1.3 μ m fluoride fibre laser", *Electr. Lett.* 24, pp. 28-29, 1988
7. M.C.Brierley and P.W.France, "Continuous wave lasing at 2.7 μ m in an erbium-doped fluorozirconate fibre", *Electron. Lett.*, 24, pp. 935-936, 1988
8. J.E. Townsend, S.B. Poole, and D.N. Payne, "Solution-doping technique for fabrication of rare-earth doped optical fibres", *Electron. Lett.* 23, pp. 329-331, 1987.
9. S.B. Poole, D.N. Payne, and M.E. Fermann, "Fabrication of low-loss optical fibre containing rare-earth ions," *Electron. Lett.* 21, pp. 737-738, 1985
10. D.C. Hanna, R.M. Percival, I.R. Perry, R.G. Smart, P.J. Suni, J.E. Townsend, and A.C. Tropper, "Continuous-wave oscillation of a monomode ytterbium-doped fibre laser", *Electron. Lett.* 24, pp. 1111-1113, 1988

11. D.C. Hanna, "Physics of fibre lasers", paper TG2, Lasers 88, Lake Tahoe, 1988
12. J.R. Armitage, R. Wyatt, B.J. Ainslie, and S.P. Craig-Ryan, "Highly efficient 980nm operation of an Yb^{3+} -doped silica fibre laser", Electron. Lett. 25, pp. 298-299, 1989
13. D.C. Hanna, I.R. Perry, R.G. Smart, P.J. Suni, and A.C. Tropper, "Efficient Superfluorescent emission at 974nm and 1040nm from an Yb-doped fibre", Opt. Comm. 72, pp. 230-234, 1989
14. R.I. Laming, M.C. Farries, P.R. Morkel, L. Reekie, D.N. Payne, P.L. Scrivener, F. Fontana and A. Righetti, "Efficient pump wavelengths of erbium-doped fibre optical amplifier", Electr. Lett. 25, pp. 12-14, 1989
15. H.C. Lefevre, "Single-mode fiber fractional wave devices and polarisation controllers", Electron. Lett. 16, pp. 778-780, 1980
16. D.C. Hanna, R.M. Percival, I.R. Perry, R.G. Smart, P.J. Suni, J.E. Townsend, and A.C. Tropper, "Continuous-wave oscillation of a monomode thulium-doped silica fibre laser", Electr. Lett., 24, pp. 1222-1223, 1988
17. D.C. Hanna, R.M. Percival, I.R. Perry, R.G. Smart, P.J. Suni and A.C. Tropper, "Thulium-doped monomode silica fiber as a laser medium", Paper TUPl, CLEO '89, Baltimore, April 1989
18. D.C. Hanna, R.M. Percival, I.R. Perry, R.G. Smart, P.J. Suni and A.C. Tropper, "Continuous-wave oscillation of a monomode thulium-doped silica fibre laser", Paper WE3, Topical Meeting on Tunable Solid State Lasers, North Falmouth, Cape Cod, May 1989
19. C.A. Millar, S.R. Mallinson, B.J. Ainslie and S.P. Craig, "Photochromic behaviour of thulium-doped silica optical fibres", Electr. Lett., 24, pp. 590-591, 1988
20. E. Snitzer, H. Po, F. Hakimi, R. Tumminelli and B.C. McCollum, "Double clad, offset core Nd fiber laser", postdeadline paper PD-5, OFC'88, New Orleans, 1988
21. L. Reekie, R.J. Mears, S.B. Poole, and D.N. Payne "A Pr^{3+} -doped single-mode fibre laser," IEE Symposium, London, 1986.
22. R.M. Percival, M.W. Phillips, D.C. Hanna and A.C. Tropper, "Characterization of spontaneous and stimulated emission from Praseodymium (Pr^{3+}) ions doped into a silica-based monomode optical fiber, IEEE J. Quant. Electr., to be published
23. L. Esterowitz, R. Allen, M. Krueer, F. Bartoli, L.S. Goldberg, H.P. Janssen, A. Linz, and V.O. Nicolai, "Blue light emission by a $\text{Pr}:\text{LiYF}$ laser operated at room temperature," J. Appl. Phys. 48, pp. 650-652, 1977
24. A. Yariv, S.P.S. Porto, and K. Nassau, "Optical maser emission from trivalent praseodymium in calcium tungstate," J. Appl. Phys. 33, pp. 2519-2521, 1962
25. B.J. Ainslie, S.P. Craig, and S.T. Davey, "The absorption and fluorescence spectra of rare earth ions in silica-based monomode fiber," J. Lightwave Technol. LT-6, pp. 287-293 1988
26. D.C. Hanna, R.M. Percival, R.G. Smart, J.E. Townsend, and A.C. Tropper, "Continuous-wave oscillation of a holmium-doped silica fibre laser", Electr. Lett. 25, pp. 593-594, 1988

27. H.W.Gandy and R.J.Ginther, "Stimulated Emission from holmium activated silicate glass", Proc IRE, 1962, 50, pp. 2113-2114, 1962
28. M.C.Brierley, P.W.France and C.A.Millar, "Lasing at 2.08 μ m and 1.38 μ m in a holmium-doped fluoro-zirconate fibre laser", Electron. Lett. 24, pp. 539-540, 1988
29. W.F.Krupke, "Induced-emission cross-sections in neodymium laser glasses", IEEE J.Quant.Electr., QE-10, pp. 450-457 1974
30. R.Reisfeld, L.Boehm and N.Spector, "Multiphonon relaxation rates and fluorescence lifetimes for Tm³⁺ in four oxide glasses", Chem. Phys. Lett., 49, pp. 251-254, 1977

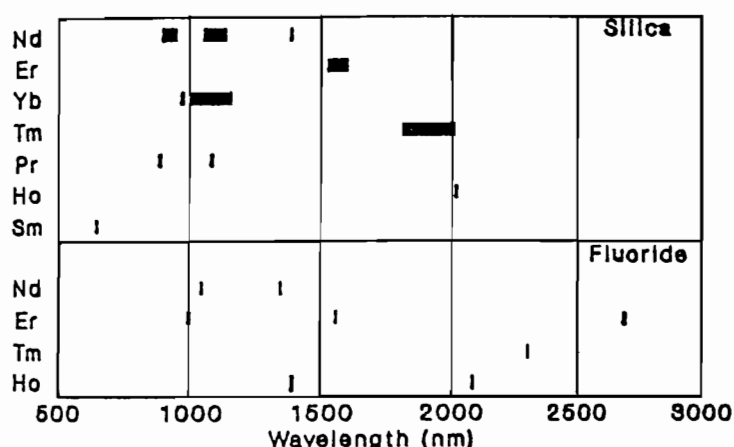


Figure 1. Wavelengths where fiber lasers have operated in silica and fluoride glass hosts. The width of each band indicated demonstrated tuning range.

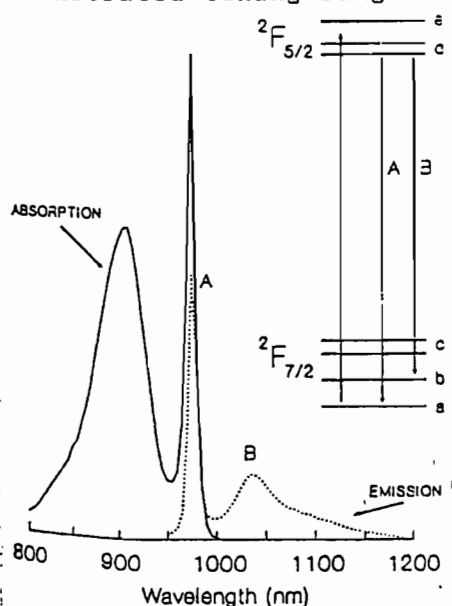


Figure 2. Yb energy levels, absorption (solid) and emission (dotted) spectra.

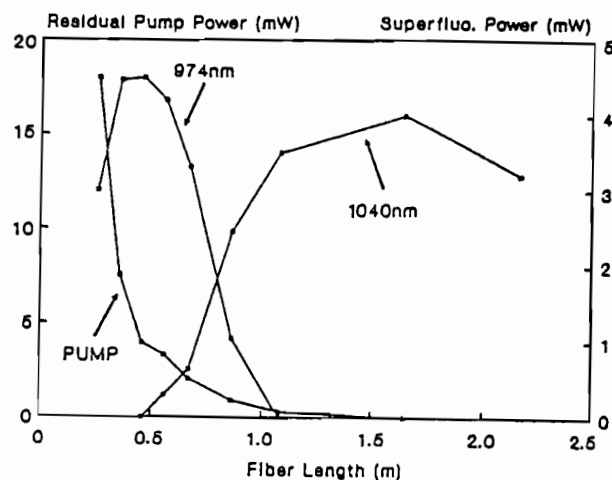


Figure 3. Superfluorescence power and residual pump power from Yb fiber versus fiber length.

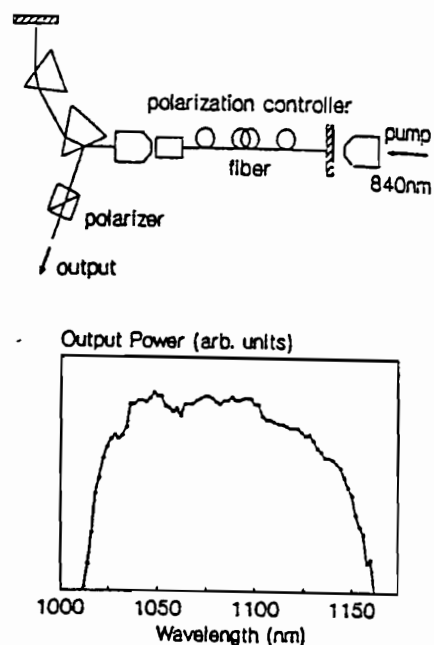


Figure 4. Resonator used to tune Yb fiber laser and resulting tuning curve.

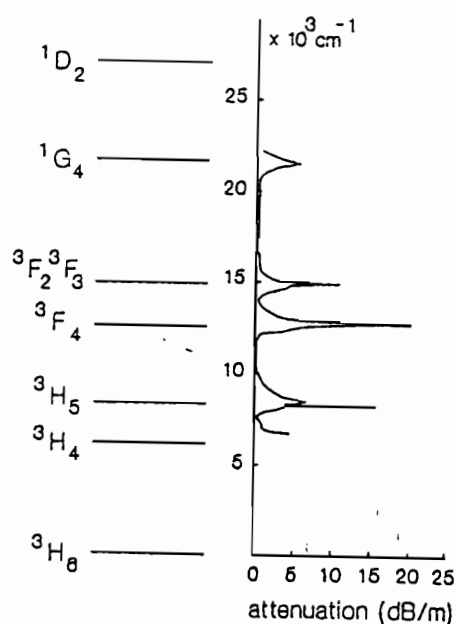


Figure 5. Energy level diagram and absorption spectrum for Tm-doped fiber.

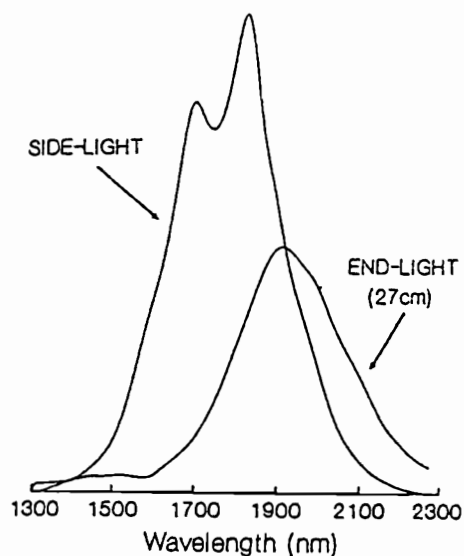


Figure 6. Fluorescence spectra from Tm fiber recorded in two ways (see text).

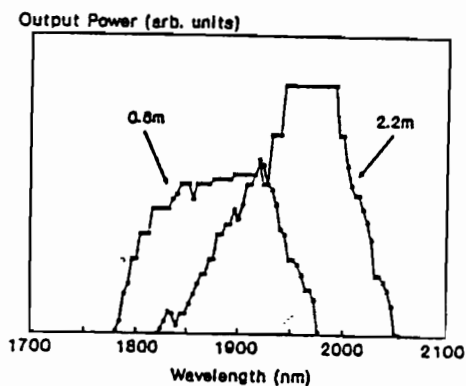


Figure 7. Tuning curves for Tm using two lengths of fiber.

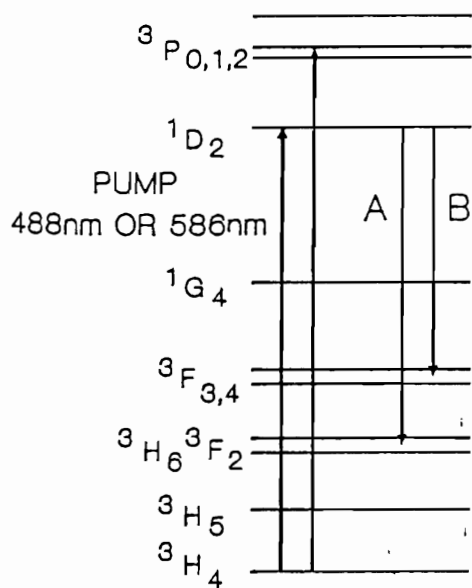


Figure 8. Energy level diagram for Pr-doped fiber. Emission spectra for transitions A and B are shown in figure 9.

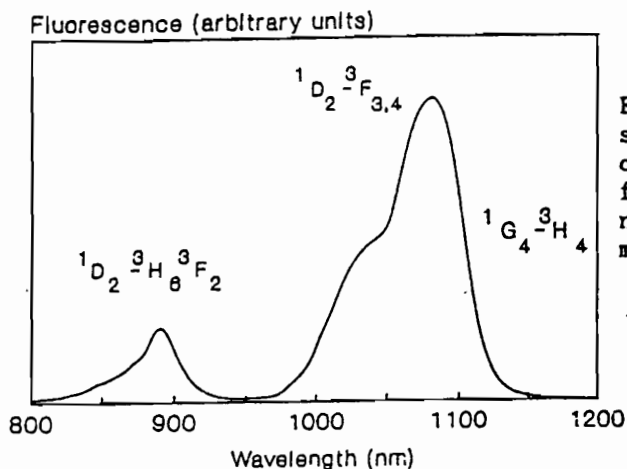


Figure 9. Pr fluorescence spectrum. The peak near 890nm corresponds to transition A in figure 8, whereas the peak near 1080nm is believed to be mainly due to transition B.

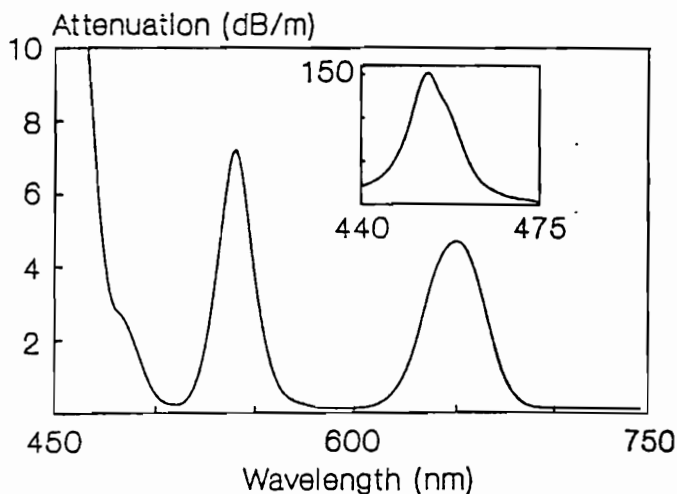


Figure 10. Ho absorption spectrum. Note change of scale for blue absorption band (inset).

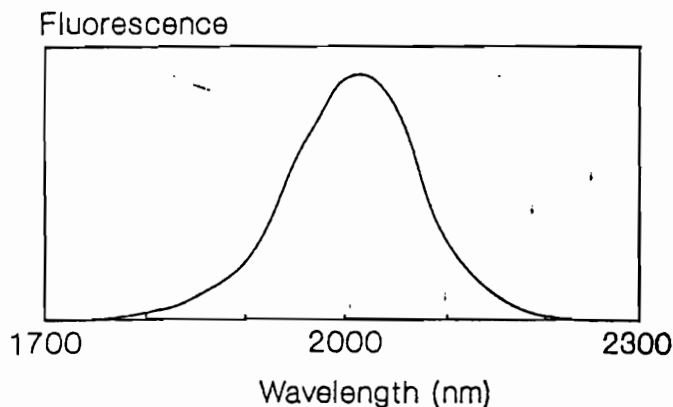


Figure 11. End light fluorescence emission from Ho fiber.